Molecular Structures of the Heavier Alkali Metal Salts of Supermesitylphosphane: A Systematic Investigation

Gerd W. Rabe,*,† Henrike Heise,† Glenn P. A. Yap,‡ Louise M. Liable-Sands,‡ Ilia A. Guzei,‡ and Arnold L. Rheingold‡

Anorganisch-chemisches Institut, Technische Universität München, Lichtenbergstrasse 4, 85747 Garching, Germany, and Department of Chemistry, University of Delaware, Newark, Delaware 19716

Received September 13, 1997

The molecular structures of the rubidium and cesium derivatives of supermesitylphosphane [i.e., (2,4,6-^{t}Bu$_3$C$_6$H$_2$)PH$_2$ = ^{t}Bu$_3$MesPH$_2$] as well as several base adducts of these are reported. Sodium hydride, potassium hydride, rubidium metal, and cesium metal react with ^{t}Bu$_3$MesPH$_2$ in tetrahydrofuran solution at room temperature to produce MPRH salts **1**−**4** [M = Na (**1**), K (**2**), Rb (**3**), Cs (**4**); R = ^{t}Bu$_3$Mes] in good yields. X-ray-quality crystals of **2** and **3** were obtained by slow evaporation of solutions of the corresponding MP(H)^{t}Bu$_3$Mes species dissolved in toluene/thf. Complex **4** was crystallized from hot toluene. On the other hand, slow evaporation of a toluene/tetrahydrofuran solution of CsP(H)^{t}Bu$_3$Mes (**4**) produces crystals of the composition {[CsP(H)^{t}Bu$_3$Mes]$_2$(μ-THF)$_{0.9}$·toluene}$_x$ (**5**). Crystallization of **4** in the presence of pyridine yields crystals of {[CsP(H)^{t}Bu$_3$Mes]$_2$(μ-pyridine)}$_x$ (**6**). Also, crystallization of complexes **3** and **4** from toluene/*N*-methylimidazole (*N*-MeIm) gives the isomorphous complexes {[RbP(H)^{t}Bu$_3$Mes]$_2$(μ-*N*-MeIm)}$_x$ (**7**) and {[CsP(H)^{t}Bu$_3$Mes]$_2$(μ-*N*-MeIm)}$_x$ (**8**), respectively. However, crystallization of **4** from toluene in the presence of bidentate or polydentate bases such as dimethoxyethane or pentamethyldiethylenetriamine does not result in incorporation of these bases into the lattice. Instead, the toluene solvate {[CsP(H)^{t}Bu$_3$Mes]$_2$(η^3-toluene)$_{0.5}$}$_x$ (**9**) is obtained. On the other hand, crystallization of **4** from toluene/ethylenediamine gives the base adduct {[CsP(H)^{t}Bu$_3$Mes]$_2$(μ-ethylenediamine)}$_x$ (**10**). Complex **3** crystallizes in the triclinic space group $P\bar{1}$. Crystal data for **3** at 218 K: a = 6.71320(10) Å, b = 10.5022(2) Å, c = 14.9733(3) Å, α = 91.3524(13)°, β = 102.5584(13)°, γ = 107.7966(14)°; Z = 1; R_1 = 6.55%. Complex **4** crystallizes in the triclinic space group $P\bar{1}$. Crystal data for **4** at 223 K: a = 7.0730(14) Å; b = 10.395(2) Å; c = 14.933(2) Å; α = 81.97(1)°; β = 76.35(2)°; γ = 71.824(14)°; Z = 1; R_1 = 4.56%. Complex **5** crystallizes in the monoclinic space group $P2_1/c$. Crystal data for **5** at 243 K: a = 15.039(2) Å; b = 16.152(3) Å; c = 20.967(5) Å; β = 91.53(2)°; Z = 4; R_1 = 4.83%. Complex **6** crystallizes in the orthorhombic space group *Pbcn*. Crystal data for **6** at 298 K: a = 14.686(2) Å; b = 21.295(5) Å; c = 28.767(5) Å; Z = 8; R_1 = 5.61%. Complex **7** crystallizes in the orthorhombic space group *Pbcn*. Crystal data for **7** at 218 K: a = 14.5533(2) Å; b = 21.4258(5) Å; c = 28.5990(5) Å; Z = 8; R_1 = 4.61%. Complex **8** crystallizes in the orthorhombic space group *Pbcn*. Crystal data for **8** at 219 K: a = 14.6162(2) Å; b = 21.3992(3) Å; c = 28.7037(2) Å; Z = 8; R_1 = 3.57%. Complex **9** crystallizes in the triclinic space group $P\bar{1}$. Crystal data for **9** at 293 K: a = 11.147(4) Å; b = 14.615(4) Å; c = 14.806(5) Å; α = 70.57(3)°; β = 71.85(3)°; γ = 72.93(2)°; Z = 2; R_1 = 5.13%. Complex **10** crystallizes in the triclinic space group $P\bar{1}$. Crystal data for **10** at 173 K: a = 10.5690(4) Å; b = 15.0376(5) Å; c = 15.3643(5) Å; α = 111.8630(10)°; β = 100.4120(10)°; γ = 97.4820(2)°; Z = 2; R_1 = 4.87%. A common feature of the molecular structures of complexes **2**−**10** is an infinitely extended polymeric ladder framework in the solid state. Both solution and solid-state NMR data are presented.

Introduction

Alkali metal salts of phosphorus-containing compounds continue to be of interest because of their synthetic value as transfer reagents and the structural diversity of their solid-state structures. Among the alkali metal derivatives of phosphides of the general formulas M[PR$_2$] and M[PRH], the lithium derivatives represent the vast majority of characterized species.[1] Only a few heavier alkali metal congeners of *molecular* sodium and potassium phosphide derivatives have been structurally characterized.[1k,2]

In contrast, several reports on solid-state phases of heavier congeners of alkali metal polyphosphides are found in the literature—most of them by von Schnering and co-workers. Numerous binary alkali metal polyphosphides containing isolated Zintl anion species of the general formulas M$^I_4$P$_6$,[3] M$^I_3$P$_7$,[4] and M$^I_3$P$_{11}$[4] and tetralkylammonium derivatives of these[5] (M^I = K−Cs) have been structurally characterized since the early 1970s.

Alkali metal salts of organophosphorus compounds play an important role as potential transfer agents. In particular, alkali metal salts of sterically demanding [PRH] anions are of importance since they are reactive transfer agents toward the formation of phosphinidene complexes or systems that might serve as suitable precursors for generating phosphinidene species. This was demonstrated previously for early transition metal[6] and main group element[7] systems and for actinide complexes.[8] The importance of alkali metal phosphides has led to

† Technische Universität München.
‡ University of Delaware.

S0020-1669(97)01178-6 CCC: $15.00
Published on Web 08/06/1998

considerable interest in their solid-state structures.[1] These structural data demonstrate that alkali metal phosphide reagents typically tend to form complexes that are aggregated to different degrees. Furthermore, solvation of the alkali metal cations by classical Lewis bases (e.g., tetrahydrofuran) is typically observed.

Recently, we focused our interest on the heavier congeners of alkali metal salts of a sterically demanding primary phosphane, namely "supermesitylphosphane".[9] Two lithium derivatives, namely ^{t}Bu$_3$MesP(H)Li(THF)$_3$[6] and ^{t}Bu$_3$MesP(H)Li·^{t}Bu$_3$MesLi,[1h] were characterized previously. An X-ray crystal structure has only been reported on the latter one. Besides this report, a limited number of other structure determinations on lithium derivatives of primary phosphanes have appeared.[1a,i,o,p,r]

Earlier we reported the molecular structure of the base-free potassium derivative of supermesitylphosphane, [KP(H)^{t}Bu$_3$Mes]$_x$, which was found to exhibit parallel extensions of an infinitely extended, centrosymmetric K−P ladder structure, with each supermesityl ring coordinated to an adjacent potassium cation.[10] Surprisingly, no donor solvent was found to be coordinated to the potassium cation although crystals were grown in the presence of a donor solvent (e.g., tetrahydrofuran and pyridine), indicating that the intramolecular interaction between the aromatic system and the alkali metal cation must be exceptionally strong. The ladder-type arrangement in [KP(H)^{t}Bu$_3$Mes]$_x$ differs significantly from the earlier reported twisted one-dimensional Li−P ladder-type structure in Li(thf)P(H)Cy (Cy = cyclohexyl).[1o]

We continued our studies by employing the sterically demanding terphenyl ligand Dmp (Dmp- = 2,6-dimesitylphenyl) as a substituent on phosphorus. Our efforts produced crystal structure determinations of both the rubidium and the cesium derivatives of (2,6-dimesitylphenyl)phosphane.[11] The rubidium derivative was found to exhibit a cubic arrangement composed of four rubidium atoms and four DmpP(H)− ligands. In contrast, the cesium derivative is composed of the cation/anion pair $Cs^+Cs_2[P(H)Dmp]_3^-$, which results in formation of an infinitely extended polymeric two-dimensional network.

Further studies in this area of chemistry have focused on the solid-state structures of different base adducts of a potassium salt of an asymmetrically substituted *secondary* phosphane, namely KP(^{t}Bu)Ph, which were found to exhibit infinitely extended polymeric K−P ladder-type structures as well.[12]

We are now investigating the accessibility as well as structural aspects of the heavier congeners of alkali metal salts of sterically demanding supermesitylphosphane. The focus of our interest is to examine structural changes that might result from alkali metal cations larger than potassium and, additionally, to study the influence of donor solvent effects on the molecular structure of the ribbon-like polymer. Interestingly, there are no reports in the literature on the synthesis, isolation, and characterization of rubidium and cesium salts of primary phosphanes.[13]

Here we report the molecular structural determinations of several different rubidium and cesium derivatives of supermesitylphosphane, thus representing a first report on molecular structures of organometallic rubidium and cesium salts of a primary phosphane, except for our earlier work[11] in this relatively undeveloped area of chemistry. As a matter of fact, a comparison of phosphide derivatives of the heavier alkali metals as well as the influence of different donor solvents has not yet been possible, which is mainly a consequence of the fact that, so far, the heavier congeners of the alkali metals have received relatively little attention compared with the ubiquitous lithium derivatives.[1] However, heavier alkali metal salts of phosphanes are of importance due to their enhanced reactivity compared with their lithium counterparts and also with respect to the structural diversity found in their solid-state structures.

Experimental Section

The compounds described below were handled under nitrogen using Schlenk double-manifold, high-vacuum, and glovebox (M. Braun, Labmaster 130) techniques. Solvents were dried and physical measurements were obtained by following typical laboratory procedures. ^{t}Bu$_3$MesPH$_2$ was prepared according to the literature.[9] LiP(H)^{t}Bu$_3$Mes(THF)$_3$ was prepared according to earlier reports.[6] Sodium hydride, potassium hydride, Rb and Cs metals, pyridine, ethylenediamine, and

(1) (a) Bartlett, R. A.; Olmstead, M. M.; Power, P. P.; Sigel, G. A. *Inorg. Chem.* **1987**, *26*, 1941. (b) Bartlett, R. A.; Olmstead, M. M.; Power, P. P. *Inorg. Chem.* **1986**, *25*, 1243. (c) Hope, H.; Olmstead, M. M.; Power, P. P.; Xu, X. *J. Am. Chem. Soc.* **1984**, *106*, 819. (d) Bartlett, R. A.; Dias, H. V. R.; Hope, H.; Murray, B. D.; Olmstead, M. M.; Power, P. P. *J. Am. Chem. Soc.* **1986**, *108*, 6921. (e) Hitchcock, P. B.; Lappert, M. F.; Power, P. P.; Smith, S. J. *J. Chem. Soc., Chem. Commun.* **1984**, 1669. (f) Hey-Hawkins, E.; Sattler, E. *J. Chem. Soc., Chem. Commun.* **1992**, 775. (g) Rabe, G. W.; Schier, A.; Riede, J. *Acta Crystallogr.* **1996**, *A52*, 1350. (h) Kurz, S.; Hey-Hawkins, E. *Organometallics* **1992**, *11*, 2729. (i) Niediek, K.; Neumüller, B. *Z. Anorg. Allg. Chem.* **1993**, *619*, 885. (j) Hey, E.; Hitchcock, P. B.; Lappert, M. F.; Rai, A. K. *J. Organomet. Chem.* **1987**, *325*, 1. (k) Driess, M.; Huttner, G.; Knopf, N.; Pritzkow, H.; Zsolnai, L. *Angew. Chem., Int. Ed. Engl.* **1995**, *34*, 316. (l) Driess, M.; Rell, S.; Pritzkow, H.; Janoschek, R. *J. Chem. Soc., Chem. Commun.* **1996**, 305. (m) Driess, M.; Pritzkow, H.; Martin, S.; Rell, S.; Fenske, D.; Baum, G. *Angew. Chem., Int. Ed. Engl.* **1996**, *35*, 986. (n) Jones, R. A.; Stuart, A. L.; Wright, T. C. *J. Am. Chem. Soc.* **1983**, *105*, 7459. (o) Hey-Hawkins, E.; Kurz, S. *Phosphorus, Sulfur, Silicon* **1994**, *90*, 281. (p) Hey, E.; Weller, F. *J. Chem. Soc., Chem. Commun.* **1988**, 782. (q) Becker, G.; Eschbach, B.; Käshammer, D.; Mundt, O. *Z. Anorg. Allg. Chem.* **1994**, *620*, 29. (r) Becker, G.; Eschbach, B.; Mundt, O.; Seidler, N. *Z. Anorg. Allg. Chem.* **1994**, *620*, 1381. (s) Pauer, F.; Power, P. P. In *Lithium Chemistry: A Theoretical and Experimental Overview*; Sapse, A.-M., Schleyer, P. v. R., Eds.; Wiley: New York, 1994; Chapter 9, p 361 and references therein. (t) Mulvey, R. E. *Chem. Soc. Rev.* **1991**, *20*, 167 and references therein.

(2) (a) Fermin, M. C.; Ho, J.; Stephan, D. W. *J. Am. Chem. Soc.* **1994**, *116*, 6033. (b) Aspinall, H. C.; Tillotson, M. R. *Inorg. Chem.* **1996**, *35*, 5. (c) Koutsantonis, G. A.; Andrews, P. C.; Raston, C. L. *J. Chem. Soc., Chem. Commun.* **1995**, 47. (d) Andrianarison, M.; Stalke, D.; Klingebiel, U. *Chem. Ber.* **1990**, *123*, 71. (e) Paul, F.; Carmichael, D.; Ricard, L.; Mathey, F. *Angew. Chem., Int. Ed. Engl.* **1996**, *35*, 1125.

(3) (a) Abicht, H.-P.; Hönle, W.; Schnering, H. G. v. *Z. Anorg. Allg. Chem.* **1984**, *519*, 7. (b) Schmettow, W.; Lipka, A.; Schnering, H. G. v. *Angew. Chem., Int. Ed. Engl.* **1974**, *13*, 345. (c) Schnering, H. G. v.; Meyer, T.; Hönle, W.; Schmettow, W.; Hinze, U. *Z. Anorg. Allg. Chem.* **1987**, *553*, 261. (d) Schnering, H. G. v. In *Homoatomic Rings, Chains and Macromolecules of Main-Group Elements*; Rheingold, A. L., Ed.; Elsevier: Amsterdam, 1977; Chapter 14, pp 317−348.

(4) (a) Meyer, T.; Hönle, W.; Schnering, H. G. v. *Z. Anorg. Allg. Chem.* **1987**, *552*, 69. (b) Schnering, H. G. v.; Hönle, W. *Chem. Rev.* **1988**, *88*, 3.

(5) (a) Korber, N.; Schnering, H. G. v. *Chem. Ber.* **1996**, *129*, 155. (b) Korber, N.; Daniels, J. *J. Chem. Soc., Dalton Trans.* **1996**, 1653.

(6) Hou, Z.; Breen, T. L.; Stephan, D. W. *Organometallics* **1993**, *12*, 3158.

(7) (a) Cowley, A. H.; Kilduff, J. E.; Lasch, J. G.; Mehrotra, S. K.; Norman, N. C.; Pakulski, M.; Whittlesey, B. R.; Atwood, J. L.; Hunter, W. E. *Inorg. Chem.* **1984**, *23*, 2582. (b) Leung, W.-P.; Chan, C. M. Y.; Wu, B.-M.; Mak, T. C. W. *Organometallics* **1996**, *15*, 5179.

(8) Arney, D. S.; Schnabel, C.; Scott, B. C.; Burns, C. J. *J. Am. Chem. Soc.* **1996**, *118*, 6780.

(9) (a) Cowley, A. H.; Norman, N. C.; Pakulski, M.; Becker, G.; Layh, M.; Kirchner, E.; Schmidt, M. *Inorg. Synth.* **1990**, *27*, 235. (b) Yoshifuji, M.; Shima, I.; Inamoto, N.; Hirotsu, K.; Higuchi, T. *J. Am. Chem. Soc.* **1981**, *103*, 4587.

(10) Rabe, G. W.; Yap, G. P. A.; Rheingold, A. L. *Inorg. Chem.* **1997**, *36*, 1990.

(11) Rabe, G. W.; Kheradmandan, S.; Liable-Sands, L. M.; Guzei, I. A.; Rheingold, A. L. *Angew. Chem.* **1998**, *37*, 1404.

(12) Rabe, G. W.; Kheradmandan, S.; Heise, H.; Liable-Sands, L. M.; Guzei, I. A.; Rheingold, A. L. *Main Group Chem.*, in press.

(13) Allen, F. H.; Davies, J. E.; Galloy, J. J.; Johnson, O.; Kennard, O.; Macrae, C. F.; Mitchell, E. M.; Mitchell, G. F.; Smith, J. M.; Watson, D. G. *J. Chem. Inf. Comput. Sci.* **1991**, *31*, 187.

redistilled *N*-methylimidazole were purchased from Aldrich. UV−vis spectra were recorded on a Perkin-Elmer Lambda 2 instrument. Solution NMR spectra were recorded on a JMN-GX 400 instrument. The solid-state MAS NMR spectra were obtained from a Bruker MSL 300 spectrometer, operating at 121.496 and 75.468 MHz for ^{31}P and ^{13}C, respectively. The ^{13}C CP/MAS NMR spectrum was referenced externally using adamantane as a secondary chemical shift standard (the low-frequency signal was set to 29.47 ppm relative to TMS). For the ^{31}P MAS NMR spectrum $(NH_4)H_2PO_4$ (1.1 ppm vs 85% H_3PO_4) was used as an external reference. Approximately 50 mg of $[KP(H)^tBu_3Mes]_x$ was packed into a 4 mm ZrO_2 rotor with a Kel-F cap. The ^{31}P NMR spectrum was obtained at a spinning speed of 15.0 kHz (recycle delay 10 s) using proton high-power decoupling. The ^{13}C CP/MAS NMR spectrum was recorded under the following conditions: recycle delay, 8 s; contact time, 5 ms; spinning speed, 10 kHz. The decoupling window for the dipolar dephasing experiment was 50 μs.

LiP(H)^{t}Bu$_3$Mes(THF)$_3$. NMR spectra of this compound in deuterated benzene were reported earlier by Stephan and co-workers.[6] ^{1}H NMR (C_4D_8O, 400 MHz, 25 °C): δ 1.17 (s, 9H), 1.63 (s, 18H), 2.83 (d, J_{P-H} = 172 Hz, 1H), 6.90 (s, 2H). ^{31}P NMR (C_4D_8O, 161.9 MHz, 25 °C): δ −108.3 (d, J_{P-H} = 172 Hz). ^{13}C NMR (C_4D_8O, 100.4 MHz, 25 °C): δ 31.9, 32.1, 32.3, 34.7 (CH_3-C), 38.7 (CH_3-C), 119.9 (d, J = 3.3 Hz, *meta*-C), 137.3 (d, J = 1.8 Hz, *para*-C), 147.4 (d, J = 5.5 Hz, *ortho*-C), 155.0 (d, J_{C-P} = 69 Hz, *ipso*-C).

NaP(H)^{t}Bu$_3$Mes (1). In a flask equipped with a Teflon stopcock, NaH (100 mg, 4.17 mmol) and supermesitylphosphane (600 mg, 2.16 mmol) were refluxed for several hours in 20 mL of tetrahydrofuran. Removal of solvent, washing of the crude product with hexanes, extraction of the residues with toluene/tetrahydrofuran (2:1), and centrifugation, followed by crystallization at −30 °C and drying under vacuum, gave **1** as colorless crystals (325 mg, 50%). Complex **1** is soluble in tetrahydrofuran but insoluble in toluene. Anal. Calcd for $C_{18}H_{30}NaP$: C, 72.00; H, 10.07. Found: C, 71.82; H, 9.85. ^{1}H NMR (C_4D_8O, 400 MHz, 25 °C): δ 1.13 (s, 9H), 1.62 (s, 18H), 2.80 (d, J_{P-H} = 167 Hz, 1H), 6.86 (s, 2H). ^{31}P NMR (C_4D_8O, 161.9 MHz, 25 °C): δ −110.0 (d, J_{P-H} = 167 Hz). ^{13}C NMR (C_4D_8O, 100.4 MHz, 25 °C): δ 31.7, 31.8, 32.3, 34.8 (CH_3-C), 38.8 (CH_3-C), 120.0 (d, J = 2.5 Hz, *meta*-C), 136.7 (d, J = 1.8 Hz, *para*-C), 147.0 (d, J = 6.1 Hz, *ortho*-C), 155.7 (d, J_{C-P} = 74 Hz, *ipso*-C). IR (Nujol): 2378 s, 1281 s, 1260 w, 1231 m, 1210 s, 1178 w, 1164 s, 1115 w, 1072 w, 1033 vs, 980 w, 922 m, 882 s, 850 m, 804 w, 768 m, 754 m, 722 m cm^{-1}.

KP(H)^{t}Bu$_3$Mes (2). In the glovebox, addition of a solution of supermesitylphosphane (200 mg, 0.72 mmol) in 5 mL of tetrahydrofuran to a colorless suspension of KH (30 mg, 0.75 mmol) in 5 mL of tetrahydrofuran caused a slow color change to yellow. The reaction mixture was stirred for 1 h. Removal of solvent, washing of the crude product with hexanes, extraction of the residues with toluene/tetrahydrofuran (2:1), and centrifugation, followed by crystallization at −30 °C and drying under vacuum, gave **2** as yellow crystals (182 mg, 80%). Complex **2** is soluble in tetrahydrofuran but insoluble in toluene. Anal. Calcd for $C_{18}H_{30}KP$: C, 68.31; H, 9.55; K, 12.35. Found: C, 68.03; H, 9.67; K, 11.95. ^{1}H NMR (C_4D_8O, 400 MHz, 25 °C): δ 1.14 (s, 9H), 1.60 (s, 18H), 2.84 (d, J_{P-H} = 163 Hz, 1H), 6.83 (s, 2H). ^{31}P NMR (C_4D_8O, 161.9 MHz, 25 °C): δ −89.3 (d, J_{P-H} = 163 Hz). ^{13}C NMR (C_4D_8O, 100.4 MHz, 25 °C): δ 31.3, 31.4, 32.3, 34.7 (CH_3-C), 38.8 (CH_3-C), 120.1 (d, J = 1.8 Hz, *meta*-C), 135.4 (d, J = 1.8 Hz, *para*-C), 145.8 (d, J = 6.5 Hz, *ortho*-C), 158.5 (d, J_{C-P} = 78 Hz, *ipso*-C). IR (Nujol): 2358 vs, 2356 s, 1277 s, 1163 m, 1033 vs, 879 m, 752 m, 721 w, 668 w, 633 w, 594 w cm^{-1}. UV−vis (tetrahydrofuran, λ_{max}, nm (ϵ)): 402 (3270), 382 (sh, 2730), 251 (7150), 245 (7660), 237 (7760), 226 (9220).

RbP(H)^{t}Bu$_3$Mes (3) and CsP(H)^{t}Bu$_3$Mes (4). In the glovebox, addition of a solution of supermesitylphosphane (200 mg, 0.72 mmol) in 5 mL of tetrahydrofuran to 1 equiv of rubidium or cesium metal (**3**, 65 mg, 0.75 mmol; **4**, 100 mg, 0.75 mmol) in 5 mL of tetrahydrofuran caused a slow color change to yellow. The reaction mixture was stirred for 2 h. Removal of solvent, washing of the crude product with hexanes, extraction of the residues with toluene/tetrahydrofuran (4:1), and centrifugation, followed by crystallization at −30 °C and drying under vacuum gave **3** (**4**) as a bright yellow powder (**3**, 157 mg, 60%; **4**, 177 mg, 60%). Complex **3** is soluble in tetrahydrofuran but insoluble in toluene. Complex **4** is soluble in tetrahydrofuran, slightly soluble in toluene at room temperature, but very soluble in hot toluene. The cesium derivative **4** can also be recrystallized from hot toluene.

3: Anal. Calcd for $C_{18}H_{30}PRb$: C, 59.58; H, 8.33. Found: C, 59.53; H, 8.15. ^{1}H NMR (C_4D_8O, 400 MHz, 25 °C): δ 1.16 (s, 9H), 1.58 (s, 18H), 2.83 (d, $^1J_{P-H}$ = 164 Hz, 1H), 6.84 (s, 2H). ^{31}P NMR (C_4D_8O, 161.9 MHz, 25 °C): δ −82.3 (d, $^1J_{P-H}$ = 164 Hz). ^{13}C NMR (C_4D_8O, 100.4 MHz, 25 °C): δ 31.2, 31.3, 32.4, 34.7 (CH_3-C), 38.8 (CH_3-C), 120.4 (d, J = 1.8 Hz, *meta*-C), 135.8 (d, J = 1.8 Hz, *para*-C), 145.8 (d, J = 6.4 Hz, *ortho*-C), 159.4 (d, J_{C-P} = 88 Hz, *ipso*-C). IR (Nujol): 2356 s, 2327 vs, 1277 vs, 1233 w, 1181 m, 1165 s, 1153 m, 1033 vs, 876 m, 842 w, 746 m, 668 w, 630 w, 591 w, 490 m cm^{-1}. UV−vis (tetrahydrofuran, λ_{max}, nm (ϵ)): 254 (sh, 9150), 248 (10 350), 214 (50 000).

4: Anal. Calcd for $C_{18}H_{30}CsP$: C, 52.69; H, 7.37. Found: C, 52.75; H, 7.49. ^{1}H NMR (C_6D_6, 400 MHz, 25 °C): δ 1.27 (s, 9H), 1.82 (s, 18H), 3.02 (d, $^1J_{P-H}$ = 163 Hz), 7.05 (s, 2H). ^{1}H NMR (C_4D_8O, 400 MHz, 25 °C): δ 1.17 (s, 9H), 1.56 (s, 18H), 2.87 (d, $^1J_{P-H}$ = 161 Hz, 1H), 6.81 (s, 2H). ^{1}H NMR (C_5D_5N, 400 MHz, 25 °C): δ 1.38 (s, 9H), 2.04 (s, 18H), 3.89 (d, $^1J_{P-H}$ = 163 Hz, 1H), 7.34 (s, 2H). ^{31}P NMR (C_6D_6, 161.9 MHz, 25 °C): δ −65.8 (d, $^1J_{P-H}$ = 163 Hz). ^{31}P NMR (C_4D_8O, 161.9 MHz, 25 °C): δ −69.2 (d, $^1J_{P-H}$ = 161 Hz). ^{31}P NMR (C_5D_5N, 161.9 MHz, 25 °C): δ −73.1 (d, $^1J_{P-H}$ = 163 Hz). ^{13}C NMR (C_4D_8O, 100.4 MHz, 25 °C): δ 31.0, 31.1, 32.5, 34.7 (CH_3-C), 38.7 (CH_3-C), 120.6 (d, J = 1.8 Hz, *meta*-C), 135.3 (d, J = 1.8 Hz, *para*-C), 145.5 (d, J = 6.4 Hz, *ortho*-C), 162.5 (d, J_{C-P} = 82 Hz, *ipso*-C). ^{13}C NMR (C_5D_5N, 100.4 MHz, 25 °C): δ 31.0, 31.1, 32.4, 34.5 (CH_3-C), 38.8 (CH_3-C), 120.9 (d, J = 1.8 Hz, *meta*-C), 145.7 (d, J = 6.0 Hz, *ortho*-C), 161.1 (d, J_{C-P} = 81 Hz, *ipso*-C). The *para*-carbon atom of complex **4** could not be found in pyridine-d_5. Presumably, it is covered by the *para*-carbon resonance of the deuterated solvent (t, δ = 135.5 ppm). Also, due to the limited solubility of CsP(H)^{t}Bu$_3$Mes in aromatic solvents, no signals could be detected in the ^{13}C NMR spectrum of **4** in C_6D_6 at room temperature. IR (Nujol): 2359 vs, 2341 s, 1277 s, 1154 m, 1031 s, 877 w, 721 m, 668 s, 594 w cm^{-1}. UV−vis (tetrahydrofuran, λ_{max}, nm (ϵ)): 254 (sh, 13 150), 248 (14 500), 214 (90 000).

General Aspects of X-Ray Data Collection, Structure Determination, and Refinement for Complexes 3−10. Crystal data, data collection, and refinement parameters are given in Table 1. Suitable crystals for single-crystal X-ray diffraction were selected and mounted in nitrogen-flushed, thin-walled glass capillaries. Graphite-monochromated Mo Kα radiation was used (λ = 0.710 73 Å). The data for **3**, **7**, **8**, and **10** were collected on a Siemens P4 diffractometer equipped with a SMART CCD detector.

No evidence of symmetry higher than triclinic was observed in the diffraction data for **3**, **4**, **9**, and **10**, and the systematic absences in the diffraction data are uniquely consistent for the reported space groups for **5**−**8**. *E* statistics suggested the centrosymmetric space group option $P\bar{1}$ for **3**, **4**, **9**, and **10**, which yielded chemically reasonable and computationally stable results of refinement. The structures were solved using direct methods, completed by subsequent difference Fourier syntheses and refined by full-matrix least-squares procedures. Semiempirical ellipsoid absorption corrections were applied to **5**, **6**, and **9** but were not required for **3**, **4**, **7**, **8**, and **10** because the integrated ψ-scan intensity data were less that 10%.

The molecules in **3** and **4** and the bridging toluene of **9** lie on an inversion center, with the methyl carbon atom of **9**, C(40), equally disordered over two positions. The tetrahydrofuran molecule in **5** was refined to a partial occupancy of 0.90. A solvent molecule of toluene was located in the asymmetric unit of **5**; the methyl carbon atom was severely disordered, and two positions were located and refined, with an occupancy distribution of 55/45. The carbon atoms of toluene were refined isotropically, and the hydrogen atoms were ignored. The methyl carbon atoms on one of the *tert*-butyl groups in **5** [C(32), C(33), and C(34)] and **6** [C(30), C(31), and C(32)] are disordered over two positions with an occupancy distribution of 50/50 and 55/45, respectively. One of the nitrogen atoms and one of the carbon atoms of the bridging ethylenediamine in **10** are disordered over two positions with an occupancy distribution of 55/45 and were refined isotropically. All

Table 1. Crystallographic Data for Complexes **3**−**10**[a]

	3	**4**	**5**	**6**	**7**	**8**	**9**	**10**
formula	$C_{36}H_{60}P_2Rb_2$	$C_{36}H_{60}Cs_2P_2$	$C_{46.6}H_{75.2}Cs_2O_{0.9}P_2$	$C_{41}H_{65}Cs_2NP_2$	$C_{40}H_{66}N_2P_2Rb_2$	$C_{40}H_{66}Cs_2N_2P_2$	$C_{39.5}H_{63.5}Cs_2P_2$	$C_{38}H_{68}Cs_2N_2P_2$
fw	725.72	820.60	977.63	899.70	807.83	902.71	866.16	880.7
crystal system	triclinic	triclinic	monoclinic	orthorhombic	orthorhombic	orthorhombic	triclinic	triclinic
space group	$P\bar{1}$	$P\bar{1}$	$P2_1/c$	*Pbcn*	*Pbcn*	*Pbcn*	$P\bar{1}$	$P\bar{1}$
a (Å)	6.71320(10)	7.0730(14)	15.039(2)	14.686(2)	14.5533(2)	14.6162(2)	11.147(4)	10.5690(4)
b (Å)	10.5022(2)	10.395(2)	16.152(3)	21.295(5)	21.4258(5)	21.3992(3)	14.615(4)	15.0376(5)
c (Å)	14.9733(3)	14.933(2)	20.967(5)	28.767(5)	28.5990(5)	28.7037(2)	14.806(5)	15.3643(5)
α (deg)	91.3524(13)	81.97(1)					70.57(3)	111.8630(10)
β (deg)	102.5584(13)	76.35(2)	91.525(15)				71.85(3)	100.4120(10)
γ (deg)	107.7966(14)	71.824(14)					72.93(2)	97.4820(2)
V (Å^3)	976.49(4)	1011.1(3)	5091.6(16)	8997(3)	8917.6(4)	8977.8(2)	2112.5(12)	2176.1(1)
Z	1	1	4	8	8	8	2	2
D_{calcd} (g cm^{-3})	1.234	1.348	1.275	1.328	1.203	1.336	1.362	1.344
temp (K)	218(2)	223(2)	243(2)	298(2)	218(2)	219(2)	293(2)	173(2)
μ_{calcd} (cm^{-1})	26.08	19.02	15.23	17.17	22.93	17.22	18.25	17.74
$R(F)$ (%)	6.55	4.56	4.83	5.61	4.61	3.57	5.13	4.87
$R_w(F^2)$ (%)	14.66	12.33	12.62	11.53	9.03	10.26	9.47	14.08

[a] The quantity minimized was $R_w(F^2) = \sum[w(F_o^2 - F_c^2)^2]/\sum[(wF_o^2)^2]^{1/2}$, $R = \sum\Delta/\sum(F_o)$, $\Delta = |(F_o - F_c)|$.

other non-hydrogen atoms were refined with anisotropic displacement parameters. The hydrogen atoms on the phosphorus atoms in **4**, **5**, and **9** were located from the difference map, the P−H distances were fixed, and in **4** and **5** the thermal parameters were constrained. The hydrogen atoms on the phosphorus atoms in **3**, **6**, **7**, **8**, and **10** could not be located from the difference map and were ignored. All other hydrogen atoms were treated as idealized contributions.

All software sources of the scattering factors are contained in the SHELXTL (5.3) program library (G. M. Sheldrick, Siemens XRD, Madison, WI).

Results and Discussion

Syntheses. Reactions of sodium hydride and potassium hydride with 1 equiv of supermesitylphosphane in tetrahydrofuran solution at room temperature (KH) or under refluxing conditions (NaH) give complexes of the general composition MP(H)^{t}Bu$_3$Mes (M = Na (**1**), K (**2**)) in good yields. Reactions of rubidium and cesium metals with 1 equiv of supermesitylphosphane in tetrahydrofuran solution at room temperature give yellow RbP(H)^{t}Bu$_3$Mes (**3**) and CsP(H)^{t}Bu$_3$Mes (**4**), respectively. The sodium, potassium, and also the rubidium derivatives of ^{t}Bu$_3$MesPH$_2$ were found to be insoluble in hexanes as well as in aromatic solvents. In contrast, the cesium salt exhibits a limited solublity in aromatic solvents at room temperature and was furthermore found to be well soluble in hot toluene. Possibly, a soft−soft interaction between the polarizable cesium cation and the aromatic solvent is the cause of this rather surprising behavior. All of the salts dissolve easily in a toluene/tetrahydrofuran mixture at room temperature. We were able to obtain single crystals of the potassium and rubidium derivatives (**2** and **3**) by slow evaporation of this solvent mixture at ambient temperature. Suitable crystals of the cesium analogue **4** were obtained by slow cooling of a hot toluene solution of **4** to ambient temperature (absence of tetrahydrofuran). It is to be noted that—so far—we have been unable to obtain single-crystalline material suitable for an X-ray crystal structural determination of the sodium derivative **1** as well as the previously reported LiP(H)^{t}Bu$_3$Mes(THF)$_3$.[6]

Scheme 1 shows the reactants discussed in this work together with the structural numbers of the products, thereby making it easier to follow the discussion (R = ^{t}Bu$_3$Mes).

Comparison of the Molecular Structures of [MP(H)^{t}Bu$_3$Mes]$_x$ [M = K (2), Rb (3), Cs (4)]. The molecular structures of complexes **2**−**4** can be described as polymeric M−P ladder-type units of the general formula [MP(H)^{t}Bu$_3$Mes]$_x$.[10] Surprisingly, no tetrahydrofuran molecule is found in the coordination spheres of both the potassium and rubidium cations although both sets of crystals were obtained from a toluene/tetrahydrofuran mixture. Since the isomorphous bright yellow cesium derivative [CsP(H)^{t}Bu$_3$Mes]$_x$ (**4**) is toluene soluble, suitable crystals for a structure determination of complex **4** could be obtained by slow cooling of a saturated hot toluene solution to ambient temperature.

Scheme 1

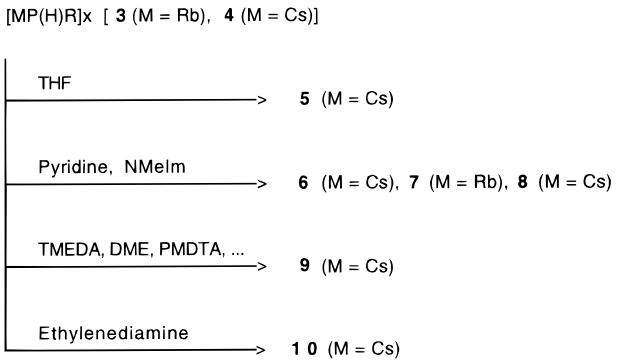

The packing diagrams of complexes **2**−**4** reveal a more extended, one-dimensional polymeric ladder-type connectivity with each phosphorus atom coordinated to three alkali metal

(14) (a) Hitchcock, P. B.; Lappert, M. F.; Lawless, G. A.; Royo, B. *J. Chem. Soc., Chem. Commun.* **1993**, 554. (b) Eaborn, C.; Hitchcock, P. B.; Izod, K.; Smith, J. D. *Angew. Chem., Int. Ed. Engl.* **1995**, *34*, 2679. (c) Eaborn, C.; Hitchcock, P. B.; Izod, K.; Smith, J. D. *Angew. Chem., Int. Ed. Engl.* **1995**, *34*, 687. (d) Eaborn, C.; Hitchcock, P. B.; Izod, K.; Jaggar, A. J.; Smith, J. D. *Organometallics* **1994**, *13*, 753. (e) Schaverien, C. J.; van Mechelen, J. B. *Organometallics* **1991**, *10*, 1704. (f) Hoffmann, D.; Bauer, W.; Schleyer, P. v. R.; Pieper, U.; Stalke, D. *Organometallics* **1993**, *12*, 1193. (g) Werner, B.; Kräuter, T.; Neumüller, B. *Organometallics* **1996**, *15*, 3746. (h) McGeary, M. J.; Cayton, R. H.; Folting, K.; Huffman, J. C.; Caulton, K. G. *Polyhedron* **1992**, *11*, 1369. (i) Fuentes, G. R.; Coan, P. S.; Streib, W. E.; Caulton, K. G. *Polyhedron* **1991**, *10*, 2371. (j) Clark, D. L.; Hollis, R. V.; Scott, B. L.; Watkin, J. G. *Inorg. Chem.* **1996**, *35*, 667. (k) Steiner, A.; Stalke, D.; *Inorg. Chem.* **1993**, *32*, 1977. (l) Niemeyer, M.; Power, P. P. *Inorg. Chem.* **1996**, *35*, 7264. (m) Neumüller, B.; Gahlmann, F. *Chem. Ber.* **1993**, *126*, 1579. (n) Klinkhammer, K. W.; Schwarz, W. *Z. Anorg. Allg. Chem.* **1993**, *619*, 1777. (o) Schmidbaur, H.; Deschler, U.; Milewski-Mahrla, B.; Zimmer-Gasser, B. *Chem. Ber.* **1981**, *114*, 608. (p) Schmidbaur, H.; Deschler, U.; Zimmer-Gasser, B.; Neugebauer, D.; Schubert, U. *Chem. Ber.* **1980**, *113*, 902. (q) Klinkhammer, K. W. *Chem.—Eur. J.* **1997**, *3*, 1418. (r) Bock, H.; Hauch, T.; Näther, C. *Organometallics* **1996**, *15*, 1527. (s) Gregory, K.; Bremer, M.; Schleyer, P. v. R.; Klusener, P. A. A.; Brandsma, L. *Angew. Chem., Int. Ed. Engl.* **1989**, *28*, 1224.

Table 2. Significant Interatomic Separations (Å) and Angles (deg) for Complexes **2**−**10**

	2 (M = K)	**3** (M = Rb)	**4** (M = Cs)	**5** (M = Cs)	**6** (M = Cs)	**7** (M = Rb)	**8** (M = Cs)	**9** (M = Cs)	**10** (M = Cs)
M−P	3.181(2)	3.381(1)	3.577(1)	3.505(3)	3.626(3)	3.518(1)	3.631(1)	3.554(3)	3.539(2)
	3.271(2)	3.433(1)	3.580(2)	3.623(3)	3.694(3)	3.571(1)	3.755(1)	3.567(4)	3.663(2)
	3.357(2)	3.504(1)	3.642(1)	3.679(3)	3.844(3)	3.700(1)	3.761(1)	3.776(4)	3.724(2)
				3.802(3)	3.853(3)	3.710(1)	3.782(1)	3.856(3)	3.832(2)
				3.967(3)	3.865(3)	3.898(1)	3.936(1)	4.039(3)	4.106(2)
				4.097(3)	3.986(3)	3.977(1)	3.993(1)	4.442(3)	4.241(2)
M(1)···C	2.884(4)	3.058(4)	3.219(5)	3.317(7)[a]	3.283(8)[a]	3.214(3)[a]	3.338(4)[a]	3.308(8)[a]	3.321(5)[a]
	3.164(4)	3.286(4)	3.423(5)	3.402(7)[a]	3.443(7)[a]	3.355(3)[a]	3.376(4)[a]	3.395(9)[a]	3.413(5)[a]
	3.197(4)	3.404(4)	3.526(5)	3.511(7)[a]	3.481(8)[a]	3.398(3)[a]	3.537(4)[a]	3.396(9)[a]	3.442(4)[a]
		3.542(5)	3.623(5)	3.685(8)[a]	3.554(8)[a]	3.478(3)[a]	3.639(4)[a]	3.417(8)[a]	3.465(5)[a]
		3.609(5)	3.685(5)	3.771(8)[a]	3.581(8)[a]	3.503(3)[a]	3.733(4)[a]	3.452(9)[a]	3.468(5)[a]
		3.670(5)	3.710(5)	3.898(8)[a]	3.617(8)[a]	3.543(3)[a]	3.766(4)[a]	3.456(9)[a]	3.477(5)[a]
P−M−P	78.22(4)	77.02(3)	79.59(3)	87.94(6)	94.28(6)	93.95(2)	95.63(3)	82.6(1)	79.19(3)
	94.33(4)	88.30(3)	86.17(3)	89.19(6)	96.11(6)	95.57(2)	96.07(3)	83.9(1)	79.29(3)
	168.96(6)	160.27(5)	162.38(4)	92.41(6)	96.63(6)	96.30(2)	97.37(3)	92.7(1)	95.46(3)
				92.59(6)	97.56(6)	98.51(2)	100.42(3)	102.1(1)	97.75(3)
				144.26(6)	129.49(6)	134.42(2)	131.44(3)	152.3(1)	144.95(3)
				160.48(6)	160.73(6)	162.22(2)	160.56(3)	165.5(1)	162.35(3)
M−P−M	85.67(4)	91.70(3)	93.83(3)	80.64(5)	73.43(5)	75.94(2)	74.86(2)	77.9(1)	82.25(3)
	101.78(4)	102.98(3)	100.41(3)	83.94(5)	74.32(5)	76.69(2)	76.57(2)	87.3(1)	84.54(3)
	168.96(6)	160.27(5)	162.38(4)	90.81(6)	83.89(6)	81.49(2)	79.58(3)	96.1(1)	96.09(3)
				92.06(6)	84.42(6)	84.54(2)	82.15(3)	97.3(1)	100.25(4)
				164.89(8)	150.85(8)	152.95(3)	149.18(4)	154.2(1)	161.49(5)
				174.15(8)	158.38(7)	161.14(3)	158.64(4)	167.1(1)	177.46(4)
M−M−M	86.15(4)	80.6(1)	81.6(1)	96.9(1)	103.49(2)	104.43(1)	103.5(1)	92.7(1)	93.8(3)
				98.6(1)	104.68(2)	104.97(1)	104.5(1)	99.0(1)	94.8(3)

[a] Only one supermesityl ring is listed.

cations [K−K−K = 86.1(1)°, Rb−Rb−Rb = 80.6(1)°, Cs−Cs−Cs = 81.6(1)°]. A comparative listing of sigificant interatomic separations of complexes **2**−**4** is given in Table 2. The interatomic M−P separations of complexes **3** and **4** (Table 2) may be compared with the corresponding distances found in M_4P_6 systems containing polyatomic anions [M = Rb, 3.476(4)−3.620(2) Å; M = Cs, 3.587(2)−3.786(1) Å].[3] Each alkali metal cation in complexes **2**−**4**, in addition to being likewise coordinated to three phosphorus atoms, appears to be coordinating to the π cloud of a neighboring supermesityl ring. The overall molecular structure of the alkali metal salts of **2**−**4** can therefore best be described as polymeric $[MP(H)^tBu_3Mes]_x$. π coordination of arene type ligands to the heavier alkali metal cations has wide precedence in the literature[14] and was also observed in the molecular structure of the potassium derivative $[KP(H)^tBu_3Mes]_x$.[10] Apparently, π interaction between the alkali metal cation and the neighboring sterically demanding supermesityl ring in complexes **2**−**4** prevents additional coordination of solvent to the metal center. It should be pointed out that the superstructures of the $[MP(H)^tBu_3Mes]_x$ polymers appear to be a ribbon of alkali metal and phosphorus atoms covered with *tert*-butyl moieties.

The alkali metal cations in complexes **2**−**4** interact to varying degrees with the aromatic ring system, which can be described as "solvating through π interaction". A closer inspection of the molecular structures of **2**−**4** (Table 2) reveals an approximate η^3-π-bonding mode in the case of the potassium derivative **2**. The highest degree of π interaction (an approximate η^6-π-bonding mode) is found in the case of the cesium derivative **4**. This observation can be rationalized in terms of an atomic size effect. According to Shannon,[15] the ionic radius increases 0.14 Å from potassium to rubidium and 0.15 Å from rubidium to cesium (given the formal coordination number 6), thereby supporting the above-mentioned assumption. C(6), in addition to being the *ipso* carbon atom, forms in all three complexes the shortest bond to M(1B) at 2.884(4) Å (**2**), 3.058(4) Å (**3**), and 3.219(5) Å (**4**).

The increasing degree of π interaction seen in complexes **2**−**4** accompanies an intensification of color going from colorless **1** over pale yellow **2** to bright yellow **3** and **4**. It should be pointed out that the alkali metal salts **3** and **4** cannot be distinguished just by simply looking at both samples. As a matter of fact, the UV−vis spectra of the rubidium species **3** and the cesium salt **4** in tetrahydrofuran solution match—except for the fact that the extinction coefficients of the cesium derivative **4** are considerably larger. On the other hand, the potassium salt **2** was seen to show only relatively weak absorption (in the near-UV region). Also, the absorption bands of **2** differ considerably from those of the heavier congeners **3** and **4**. Details are given in the Experimental Section.

In addition to an increasing degree of π interactions of the aromatic system, a certain number of nonbonding M···C interactions are found to corelate with the increasing ionic radii of the alkali metal cations: in the rubidium complex **3**, the closest Rb···C(methyl) distances are 3.567(6) Å [Rb···C(8)] and 3.643(5) Å [Rb···C(18)]. The closest Cs···C(methyl) distances for **4** are 3.720(6) Å [Cs···C(17)], 3.770(6) Å [Cs···C(9)], and 3.786(7) Å [Cs···C(8)]. These numbers are actually in the range of the weakest M−C(phenyl) distances [C(3) and C(4)] within the same molecule.

Also, it is to be noted that complexes **2**−**4** are the first representatives of discrete alkali metal derivatives of primary phosphanes stabilized only by the steric bulk of the ligand accompanied by absence of coordinating classical donor ligands (e.g., tetrahydrofuran and pyridine). This particular metal−ligand arrangement has not been observed previously in other alkali metal phosphide derivatives.

The Cs···C distances in complex **4** range from 3.219(5) to 3.710(5) Å (average 3.53 Å) and fall into the range of the corresponding distances observed in previously characterized species containing Cs···C distances, namely (a) π-carbanions,

(15) Shannon, R. D. *Acta Crystallogr.* **1976**, *A32*, 751.
(16) Gregory, K.; Bremer, M.; Schleyer, P. v. R.; Klusener, P. A. A.; Brandsma, L. *Angew. Chem., Int. Ed. Engl.* **1989**, *28*, 1224.

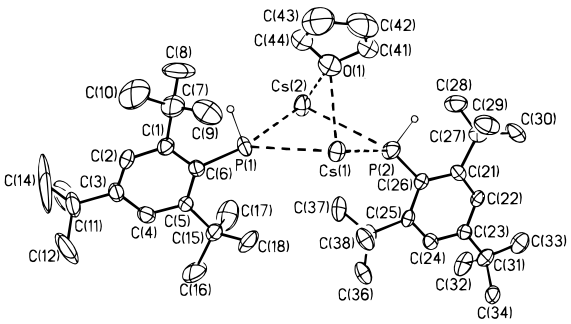

Figure 1. Molecular structure of complex **5**. Hydrogen atoms as well as the cocrystallized toluene molecule in the crystal lattice are omitted for clarity. Selected interatomic separations (Å) and angles (deg): Cs(1)−P(1) = 3.679(3), Cs(1)−P(2) = 3.623(3), Cs(1)−P(2A) = 4.097(3), Cs(2)−P(1) = 3.505(3), Cs(2)−P(2) = 3.802(3), Cs(2)−P(1B) = 3.967(3), Cs(1)−O(1) = 3.258(10), Cs(2)−O(1) = 3.325(9), Cs(1)−C(26A) = 3.317(7), Cs(1)−C(21A) = 3.402(7), Cs(1)−C(25A) = 3.511(7), Cs(1)−C(22A) = 3.685(8), Cs(1)−C(24A) = 3.771(8), Cs(1)−C(23A) = 3.898(8); O(1)−Cs(1)−P(1) = 71.1(2), O(1)−Cs(1)−P(2) = 70.3(2), O(1)−Cs(1)−P(2A) = 141.6(2), O(1)−Cs(2)−P(1) = 72.7(2), O(1)−Cs(2)−P(2) = 67.4(2), O(1)−Cs(2)−P(1B) = 130.8(2), Cs(1)−P(1)−Cs(2) = 83.94(5), Cs(1)−P(1)−Cs(2B) = 174.15(8), Cs(1)−P(2)−Cs(1A) = 90.81(6), Cs(1)−P(2)−Cs(2) = 80.64(6), Cs(2)−P(1)−Cs(2B) = 92.06(6), Cs(2)−P(2)−Cs(1A) = 164.89(8).

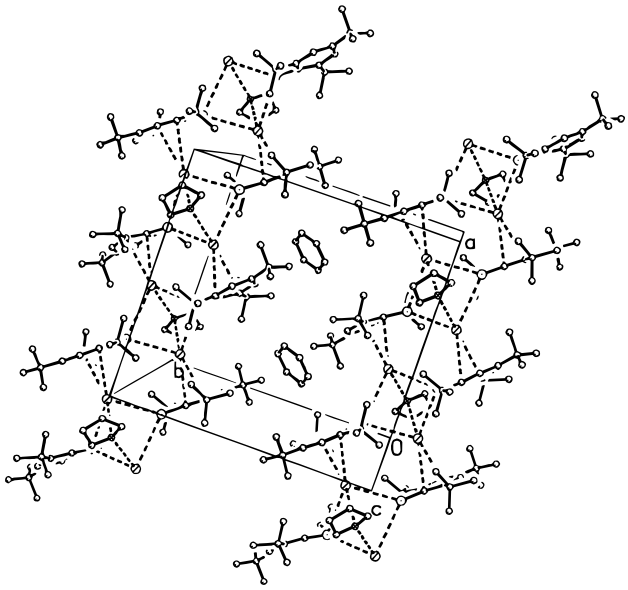

Figure 2. Unit-cell packing diagram of the cesium derivative **5** showing the parallel extensions of the ladder structure plus the cocrystallized solvent molecule.

e.g. cesiocarbazole·pmdta (average 3.43 and 3.51 Å for both isomers)[16] and (b) other π-solvates, e.g. $CsC(SiMe_3)_3 \cdot 3.5C_6H_6$ (average 3.81 Å).[17]

The environment around the phosphorus atom in complexes **2**−**4** can best be described as heavily distorted square pyramidal.[18] The deviation from ideal square pyramidal geometry can best be seen by examining the (^{t}Bu$_3$Mes)C(6)−P(1)−M(1) angles [**2**, 139.5(1)°; **3**, 138.3(2)°; **4**, 139.6(2)°]. All three angles are found to be quite small, which can be understood in terms of distortion resulting from additional π coordination of the supermesityl ring to the next alkali metal cation. A point that needs to be mentioned is that the hydrogen atoms on the phosphorus atoms in **2**−**4** tend to be coplanar with the aryl ring, leaving the lone pairs to partially conjugate with the ring.

{[CsP(H)^{t}Bu$_3$Mes]$_2$(μ-THF)$_{0.9}$.toluene}$_x$ (5). We were interested in investigating whether donor solvents can coordinate to the polymeric structures of complexes **2**−**4** and what kind of structural changes might result. Coordination of tetrahydrofuran to the metal center was found only in the case of the cesium derivative **4**, forming the polymeric cesium complex $\{[CsP(H)^tBu_3Mes]_2(\mu\text{-THF})_{0.9}\cdot\text{toluene}\}_x$ (**5**). The potassium and rubidium derivatives were found not to coordinate tetrahydrofuran under similar crystallization conditions. Complex **5** desolvates very easily upon removal of the solvent mixture. This observation is also supported by the fact that the tetrahydrofuran molecule in the X-ray crystal structure of **5** is occupied only to the 90% level. Therefore, an attempted further characterization failed—except for a crystal structure that was obtained from a crystal isolated directly from this particular solvent mixture. The molecular structure of the cesium salt **5** shows a higher effective coordination number at the metal center compared with that of the donor solvent-free complex **4**. Additional coordination of a tetrahydrofuran molecule per two CsP(H)^{t}Bu$_3$Mes units (Figures 1 and 2) is observed as a result of an atomic size effect. In the case of the cesium derivative **5**, the larger cesium cation is apparently not as well shielded by the *tert*-butyl groups of the ligand system as in the case of the potassium or rubidium derivative (**2** or **3**). Consequently, the relatively large cesium cation in complex **5** allows for additional coordination of one bridging tetrahydrofuran molecule per two cesium cations. Again, a certain amount of weak Cs···C contacts is seen to be present: the closest Cs···C(methyl) distances in **5** are 3.655(10) Å [Cs(1)···C(29)] and 3.840(9) Å [Cs(1)···C(38)]. As was observed in the case of complexes **2**−**4**, the packing diagram of complex **5** shows the expected ribbon array. Also, it is to be noted that complex **5** crystallizes with one molecule of toluene per two CsP(H)^{t}Bu$_3$Mes units in the unit-cell packing. Replacement of toluene by benzene in the crystallization process produced cell data indicating an isomorphous structure in the solid state.

{[CsP(H)^{t}Bu$_3$Mes]$_2$(μ-pyridine)}$_x$ (6) and {[MP(H)^{t}Bu$_3$Mes]$_2$(μ-*N*-MeIm)}$_x$ (M = Rb (7); M = Cs (8)). We continued our systematic study by employing different monodentate nitrogen donor solvents in the crystallization process, namely pyridine and *N*-methylimidazole (*N*-MeIm). Crystalline material suitable for an X-ray crystal structure was obtained by slow cooling of a solution of CsP(H)^{t}Bu$_3$Mes in hot toluene/pyridine to ambient temperature. The composition of this species was determined crystallographically as the pyridine adduct $[\{CsP(H)^tBu_3Mes\}_2(\mu\text{-pyridine})]_x$, **6** (Figures 3−5).

The solid-state structure of complex **6** exhibits a novel and rather peculiar asymmetric polymeric structure that is found to be quite different from the molecular structures observed for the donor solvent-free alkali metal derivatives of the general formula $[MP(H)^tBu_3Mes]_x$ (M = K−Cs) as well as the tetrahydrofuran adduct $\{[CsP(H)^tBu_3Mes]_2(\mu\text{-THF})_{0.9}\cdot\text{toluene}\}_x$ (**5**). The extended structure of **6** (Figure 4) consists of a polymeric ladder framework of cesium and phosphorus atoms with each supermesityl ligand additionally coordinated to an adjacent cesium cation via an η^6-π-interaction. As was found in the tetrahydrofuran adduct **5**, additional coordination of one bridging donor solvent molecule (pyridine) per two cesium cations is found.

(17) Eaborm, C.; Hitchcock, P. B.; Izod, K.; Smith, J. D. *Angew. Chem., Int. Ed. Engl.* **1995**, *34*, 687.

(18) A drawing of what is meant by a "square pyramidal coordination environment" for the phosphorus atom is provided in Figure 1 of ref 10.

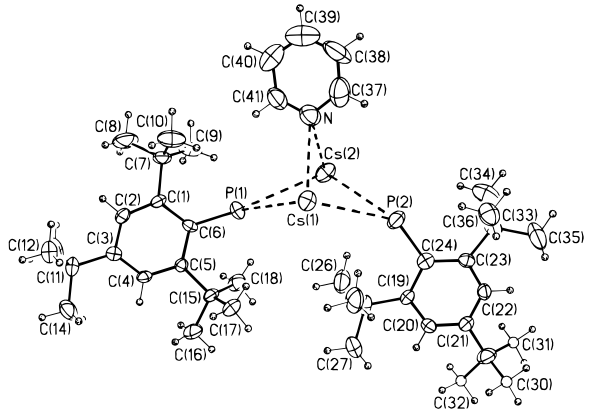

Figure 3. ORTEP diagram and numbering scheme of the asymmetric unit of $\{[CsP(H)^tBu_3Mes]_2(\mu\text{-pyridine})\}_x$, (**6**).

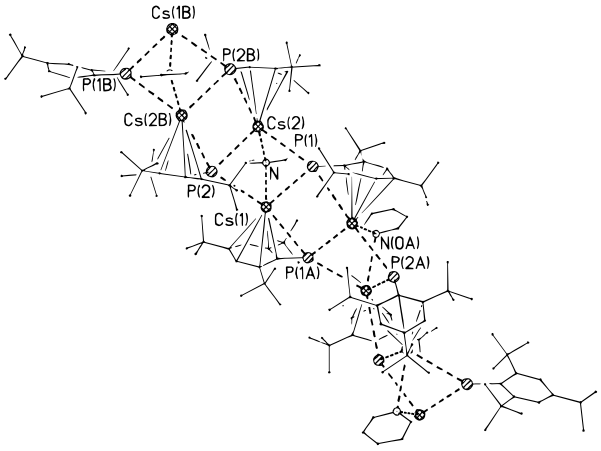

Figure 4. Unit-cell packing diagram for $\{[CsP(H)^tBu_3Mes]_2(\mu\text{-pyridine})\}_x$ (**6**) showing the infinite extensions of the chains of the polymeric framework. Selected interatomic separations (Å) and angles (deg): Cs(1)−P(1) = 3.626(3), Cs(1)−P(1A) = 3.844(3), Cs(1)−P(2) = 3.865(3), Cs(2)−P(1) = 3.853(3), Cs(2)−P(2) = 3.694(3), Cs(2)−P(2A) = 3.986(3), Cs(1)−N = 3.365(10), Cs(2)−N = 3.386(11), Cs(1)−C(6A) = 3.283(8), Cs(1)−C(5A) = 3.443(7), Cs(1)−C(1A) = 3.481(8), Cs(1)−C(4A) = 3.554(8), Cs(1)−C(2A) = 3.581(8), Cs(1)−C(3A) = 3.617(8); N−Cs(1)−P(1) = 75.7(2), N−Cs(1)−P(1A) = 115.9(2), N−Cs(1)−P(2) = 81.9(2), Cs(1)−P(1)−Cs(1A) = 84.42(6), Cs(1)−P(1)−Cs(2) = 74.32(5), Cs(1A)−P(1)−Cs(2) = 158.38(7), Cs(2)−P(2)−Cs(1) = 73.43(5), Cs(2)−P(2)−Cs(2B) = 83.89(6), Cs(1)−P(2)−Cs(2B) = 150.85(8).

In the ladder-type connectivity of **6**, each phosphorus atom is coordinated to three cesium cations with Cs−P interatomic separations ranging from 3.626(3) to 3.986(3) Å and P−Cs−P angles of 94.28(6), 96.11(6), 96.63(6), 97.56(6), 129.49(6), and 160.73(6)°. The Cs−Cs−Cs angles are 103.49(2) and 104.68(2)°.

In contrast to the infinitely extended parallel polymers of the general formula $[MP(H)^tBu_3Mes]_x$ (**2**−**4**) and the molecular structure of the tetrahydrofuran adduct **5**, a twist is observed in the infinitely extended ladder of **6**. Four asymmetric units of **6** (Figure 5) compose one full cycle of a complete structural motif that is a ribbon that twists approximately 130° in one direction and then reverses and twists equally in the opposite direction. The ribbon is centrosymmetric with inversion centers in the planes formed by P(2), Cs(2), and their symmetrical equivalents, i.e., in Figure 4, Cs(2), P(2), P(2B), and Cs(2B). A 2-fold rotational axis passes through the P(1), Cs(1), P(1A), Cs(1A) rhombus.

The observation of the formation of this unusual structure in the solid state is quite surprising in light of the fact that the tetrahydrofuran adduct **5** exhibits a one-dimensional and nontwisted polymeric structure in the crystalline state.

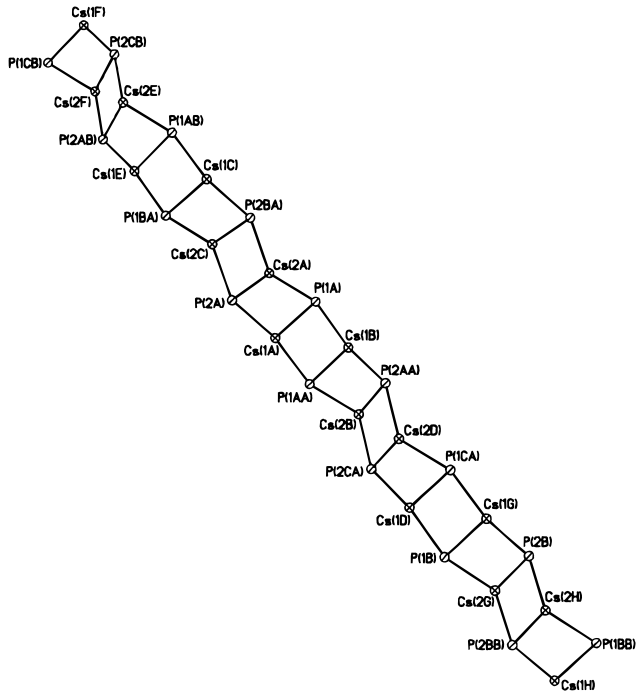

Figure 5. Ball-and-stick drawing of the Cs−P framework of complex **6**.

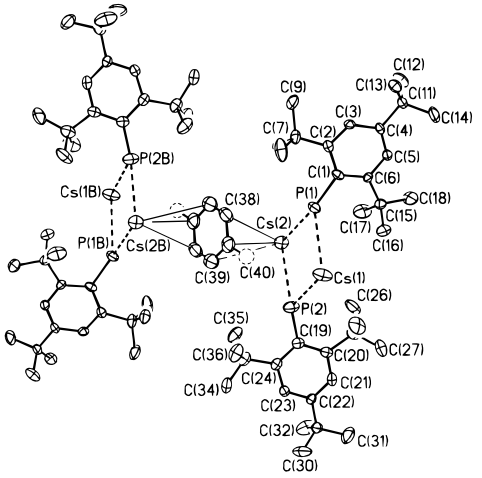

Figure 6. Molecular diagram of $\{[CsP(H)^tBu_3Mes]_2(\eta^3\text{-toluene})_{0.5}\}_x$ (**9**) showing the interaction of two dimers with the solvent molecule.

We found that pyridine does not coordinate to the potassium and the rubidium ions in complexes **2** and **3**, respectively, but coordinates only to the larger cesium ions of complex **4**, which can be rationalized in terms of an atomic size effect. It is to be noted that—besides the yellow crystals of complex **6**—we also observed formation of an orange species crystallizing from a hot tolulene/pyridine mixture. On the basis of the unit cell data,[19] it can be assumed that this species is presumably isomorphous with the tetrahydrofuran adduct **5**, although we were not able to obtain a complete data set because of decomposition of the crystal.

Using *N*-methylimidazole (*N*-MeIm) instead of pyridine as a donor solvent produces crystalline material suitable for an X-ray crystal structure of the isomorphous *N*-MeIm adducts of the

(19) Unit-cell data at 298 K: a = 15.142(1) Å; b = 16.229(4) Å; c = 20.880(3) Å; β = 90.007(9)°; V = 5133(2) Å^3.

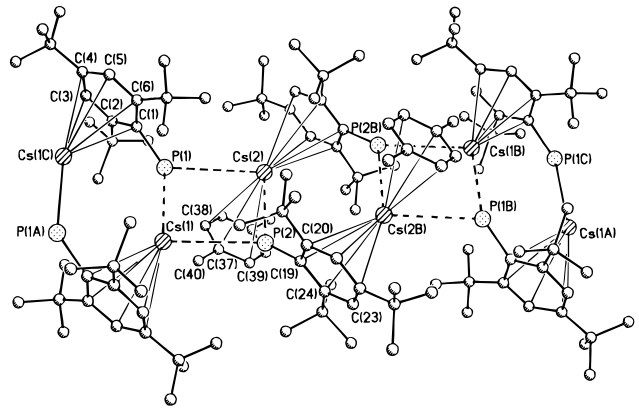

Figure 7. View of the molecular structure of $\{[CsP(H)^tBu_3Mes]_2(\eta^3\text{-toluene})_{0.5}\}_x$ (**9**) showing the different coordination environments of Cs(1) and Cs(2). Selected interatomic separations (Å) and angles (deg): Cs(1)−P(1) = 3.554(3), Cs(1)−P(2) = 3.776(4), Cs(1)−P(1A) = 4.039(3), Cs(2)−P(1) = 3.856(3), Cs(2)−P(2) = 3.567(4), Cs(2)−P(2B) = 4.442(3), Cs(1)−C(1A) = 3.308(8), Cs(1)−C(6A) = 3.395(9), Cs(1)−C(5A) = 3.396(9), Cs(1)−C(4A) = 3.417(8), Cs(1)−C(2A) = 3.452(9), Cs(1)−C(3A) = 3.456(9), Cs(2)−C(19B) = 3.465(9), Cs(2)−C(24B) = 3.478(9), Cs(2)−C(20B) = 3.494(9), Cs(2)−C(21B) = 3.522(9), Cs(2)−C(23B) = 3.523(9), Cs(2)−C(22B) = 3.585(9), Cs(2)−C(37) = 3.679(13), Cs(2)−C(38) = 3.825(14), Cs(2)−C(39) = 3.928(13); Cs(1)−P(1)−Cs(2) = 96.1(1), Cs(1)−P(1)−Cs(1A) = 77.9(1), Cs(1)−P(2)−Cs(2B) = 154.2(1), Cs(2)−P(2)−Cs(1) = 97.3(1), Cs(2)−P(2)−Cs(2B) = 87.3(1), Cs(2)−P(1)−Cs(1A) = 167.1(1), P(1)−Cs(2)−C(37) = 70.5(3), P(1)−Cs(2)−C(38) = 65.7(3), P(2)−Cs(2)−C(37) = 71.6(3), P(2)−Cs(2)−C(38) = 92.0(3).

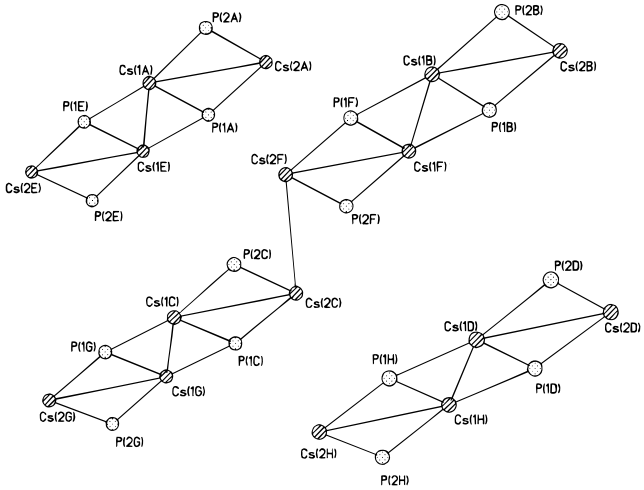

Figure 8. Ball-and-stick drawing of the Cs−P framework of **9** showing the characteristic ABB′A′ pattern.

general composition $\{[MP(H)^tBu_3Mes]_2(\mu\text{-}N\text{-MeIm})\}_x$ (M = Rb, **7**; M = Cs, **8**). Both **7** and **8** show an arrangement of the polymeric M−P framework similar to that observed in the isomorphous pyridine adduct **6**. Complexation of the rubidium derivative **3** by *N*-MeIm but not by pyridine can presumably be attributed to (a) the higher basicity and polarity of *N*-MeIm as opposed to pyridine and (b) the fact that *N*-MeIm, being a five-membered ring, is smaller than the six-membered ring system of pyridine. Significant interatomic separations and angles of the isomorphous systems **6**−**8** are listed in Table 2. On the basis of the structural data obtained so far, it can be concluded that pyridine or bases similar to pyridine yield the above-mentioned structural motif.

$\{[CsP(H)^tBu_3Mes]_2(\eta^3\text{-toluene})_{0.5}\}_x$ (9). Crystallization of **4** from toluene in the presence of bidentate or tridentate donor molecules (DME, TMEDA, DMPE, PMDETA, (−)-sparteine, phthalazine, 4,4′-bipyridine, pyrazine) results neither in their incorporation into the crystal lattice nor in coordination of these bases to a cesium cation. Instead, a toluene solvate molecule is found to be incorporated in the crystal lattice with a $[Cs_2P_2]$:toluene ratio of 2:1, thereby resulting in formation of a complex of composition $\{[CsP(H)^tBu_3Mes]_2(\eta^3\text{-toluene})_{0.5}\}_x$ (**9**) (Figures 6−9). It is interesting to note that we were unable to produce crystals of **9** by recrystallizing $CsP(H)^tBu_3Mes$ (**4**) directly from toluene. Only in the presence of bi- or tridentate bases is formation of complex **9** reproducibly observed.

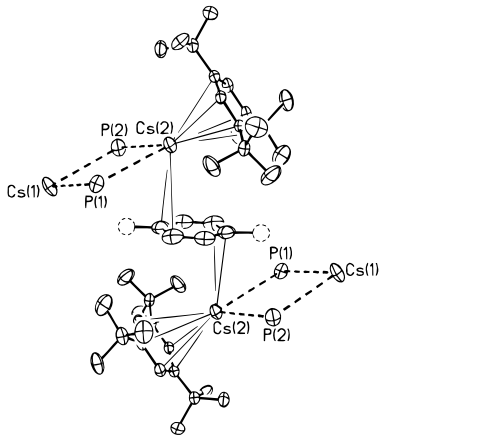

Figure 9. Bent triple-decker-type arrangement of the aromatic rings around Cs(2) in complex **9**.

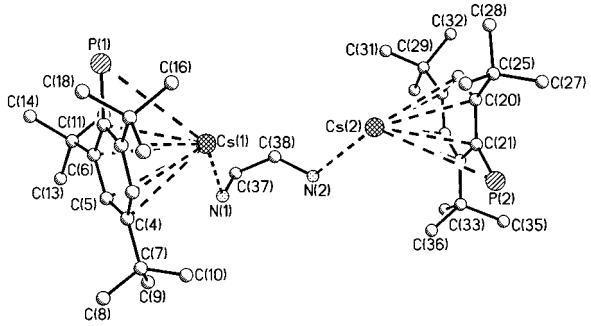

Figure 10. Molecular structure of $\{[CsP(H)^tBu_3Mes]_2(\mu\text{-ethylenediamine})\}_x$ (**10**). The preferred orientation of the disordered atoms N(1) and C(37) is shown. Selected interatomic separations (Å) and angles (deg): Cs(1)−N(1) = 3.248(11), Cs(2)−N(2) = 3.216(8), Cs(1)−P(1) = 4.106(2), Cs(1)−P(1A) = 3.539(2), Cs(1)−P(2B) = 3.832(2), Cs(2)−P(2) = 4.241(2), Cs(2)−P(1A) = 3.724(2), Cs(2)−P(2B) = 3.663(2); P(1)−Cs(1)−P(1A) = 97.75(3), P(1)−Cs(1)−P(2B) = 162.35(3), P(1A)−Cs(1)−P(2B) = 79.29(3), P(1A)−Cs(2)−P(2B) = 79.19(3), P(2)−Cs(2)−P(1A) = 144.95(3), P(2)−Cs(2)−P(2B) = 95.46(3).

The Cs−P bond distances in **9** are 3.554(3), 3.776(4), and 4.039(3) Å for Cs(1) and 3.567(4), 3.856(3), and 4.442(3) Å for Cs(2), respectively. Detailed interatomic separations and angles are given in Table 2.

The extended connectivity of **9** consists of an infinitely extended ladder which features an ABB′A′ motif (Figures 7 and 8). As can be seen from Figures 6 and 9, the parallel ladders are linked by an η^3-bonded toluene molecule, which is crystallographically disordered 50/50 between two positions with the methyl groups occupying either position half of the time. The toluene molecule, which has the function of a spacer between the individual polymers, occupies an inversion center.

There are two different types of cesium cations present in complex **9**, namely those coordinated to a $^tBu_3Mes$ phenyl ring as well as three phosphorus atoms [Cs(1)] and those exhibiting additional coordination to three carbon atoms of the solvate molecules [Cs(2)] (Figure 7). The overall coordination geom-

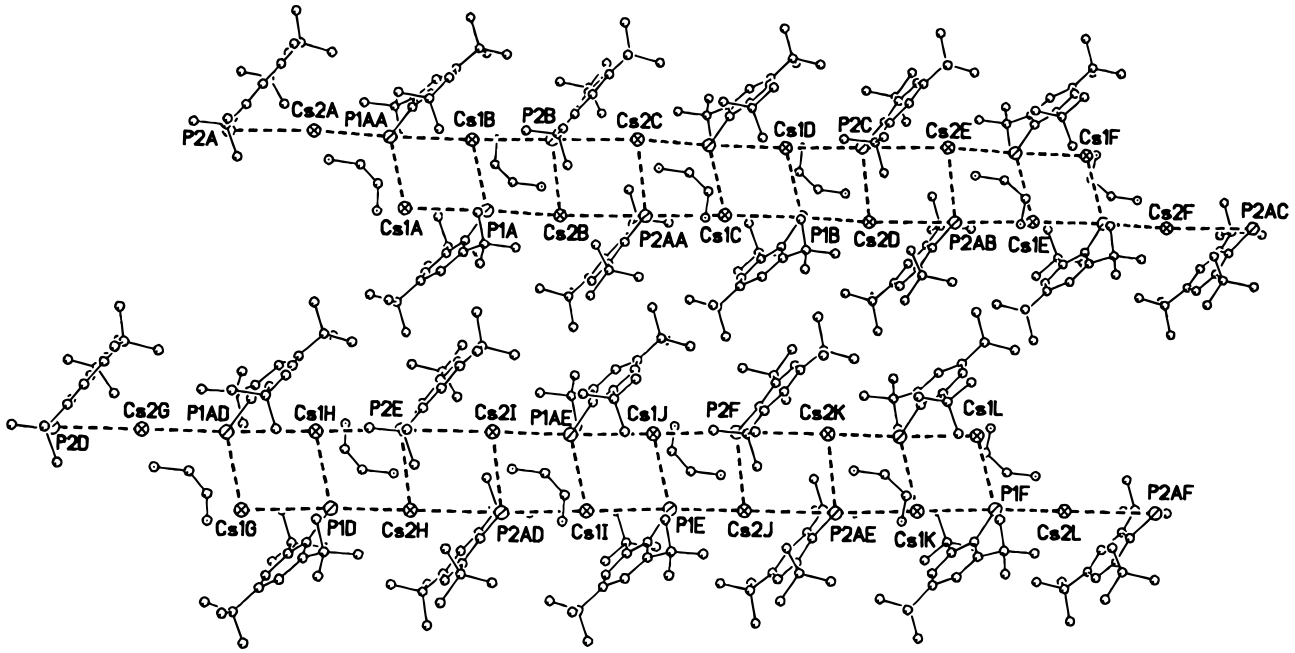

Figure 11. Unit-cell packing diagram for $\{[CsP(H)^tBu_3Mes]_2(\mu\text{-ethylenediamine})\}_x$ (**10**) showing the parallel extensions of the ladder structure.

etry around Cs(2) can best be described as a bent triple-decker complex, which is formed by two Cs(2) cations, two supermesityl rings, and one toluene molecule (Figure 9). The supermesityl ring(centroid)−Cs(2)−toluene(centroid) angle is 85.1(3)°. A similar organometallic bent triple-decker-type arrangement with a corresponding angle of 115.6(2)° was found earlier in the Cp_3Cs_2 anion.[20] Additionally, there are two reports in the literature on $[Cs_2(18\text{-crown-}6)_3]^{2+}$ cations exhibiting "club sandwich" structures.[21,22]

The average Cs(2)···C(toluene) distances in complex **9** (ranging from 3.679(13) to 3.928(13) Å) are approximately 0.3 Å longer than the distances between Cs(2) and the $^tBu_3Mes$ phenyl carbon atoms. They can be compared with the Cs(2)···C(54) distance of 6.03(1) Å in complex **5**, which is the shortest Cs···C(toluene) distance between the alkali metal cation and the cocrystallized toluene molecule in the crystal lattice. Additionally, C(28), being a methyl carbon atom of one of the *tert*-butyl groups in **9**, is seen to show a weak interaction with Cs(2) at a distance of 3.60(1) Å.

Finally, it is to be noted that employment of 2,2′-bipyridine in the crystallization process of $CsP(H)^tBu_3Mes$ produced crystals with a unit cell[23] twice as large as was obtained for complex **9**. However, the cell contents of both species were found to be identical, with twice as many molecules of **9** in the larger cell.

$\{[CsP(H)^tBu_3Mes]_2(\mu\text{-ethylenendiamine})\}_x$ (10). We continued our systematic study by recrystallizing the cesium derivative **4** from toluene in the presence of ethylenediamine. The structural motif found in $\{[CsP(H)^tBu_3Mes]_2(\mu\text{-ethylenediamine})\}_x$ (**10**) is shown in Figures 10 and 11. Again, the typical ladder-type structure common for this class of complexes is observed. In contrast to the structural motifs seen in complexes **5**−**8**, which are found to be solvated by *monodentate* bases, complex **10** is complexed by the two nitrogen atoms of the ethylendiamine ligands bridging Cs(1) and Cs(2) within the same ladder. We also attempted the crystallization of $[CsP(H)^tBu_3Mes]_x$ (**4**) from toluene in the presence of ethylene glycol ($HOCH_2CH_2OH$). In contrast to the coordinating behavior of ethylenediamine, alcoholysis of the cesium phosphide producing $^tBu_3MesPH_2$ was observed instead of coordination of the glycol to the cesium cations of the cesium phosphide.

Detailed bonding parameters of the molecular structure of **10** can be derived from Table 2. In addition to the π coordination of each supermesityl ligand to a neighboring cesium cation, a weak interaction between Cs(1) and the methyl carbon atom C(35B) [3.817(8) Å] is found to be present. Also, Cs(2) is in weak contact with carbon atom C(38) of the ethylendiamine ligand at a distance of 3.767(7) Å. One of the nitrogen atoms, namely N(1), and also carbon atom C(37) of the bidentate donor base are disordered over two positions with a ratio of 55/45.

Figure 12 shows the different kinds of ladders that occur for the structural motifs found in the cesium derivatives **4**, **5**, **6**, **8**, **9**, and **10**, in similar orientations.

Deformation of the Phenyl Rings in Complexes 2−10. Different amounts of deformation of the phenyl rings are found to be present in complexes **2**−**10**. The deviation from planarity in all cases is greatest at the *ipso* carbon atom. Therefore, the deviation from the ideal 180° plane is most readily seen by examining the deviation of the *ipso* carbon atom from the least-squares planes determined by the other five carbon atoms of these rings. The *ipso* carbon atom is elevated 0.11 Å [**2**, C(6)], 0.19 Å [**3**, C(6)], 0.20 Å [**4**, C(6)], 0.13 and 0.01 Å [**5**, C(6) and C(26)], 0.16 and 0.12 Å [**6**, C(6) and C(24)], 0.12 and 0.14 Å [**7**, C(11) and C(29)], 0.11 and 0.14 Å [**8**, C(11) and C(29)], 0.15 and 0.01 Å [**9**, C(1) and C(19)], and 0.13 and 0.02 Å [**10**,

(20) Harder, S.; Prosenc, M. H. *Angew. Chem., Int. Ed. Engl.* **1996**, *35*, 97.
(21) Vidal, J. L.; Schoening, R. C.; Troup, J. M. *Inorg. Chem.* **1981**, *20*, 227.
(22) Domasevitch, K. V.; Ponomareva, V. V.; Rusanov, E. B. *J. Chem. Soc., Dalton Trans.* **1997**, 1177.
(23) Unit-cell data at 223 K: $a = 14.8860(3)$ Å; $b = 14.8860(3)$ Å; $c = 22.3990(5)$ Å; $\alpha = 71.863(1)°$; $\beta = 73.037(1)°$; $\gamma = 70.589(1)°$; $V = 4286.79(5)$ Å^3.
(24) (a) Cowley, A. H.; Gabbaï, F. P.; Corbelin, S.; Decken, A. *Inorg. Chem.* **1995**, *34*, 5931. (b) Yoshifuji, M.; Shima, I.; Inamoto, N.; Hirotsu, K.; Higuchi, T. *Angew. Chem., Int. Ed. Engl.* **1980**, *19*, 399. (c) Cowley, A. H.; Palulski, M.; Norman, N. C. *Polyhedron* **1987**, *6*, 915.

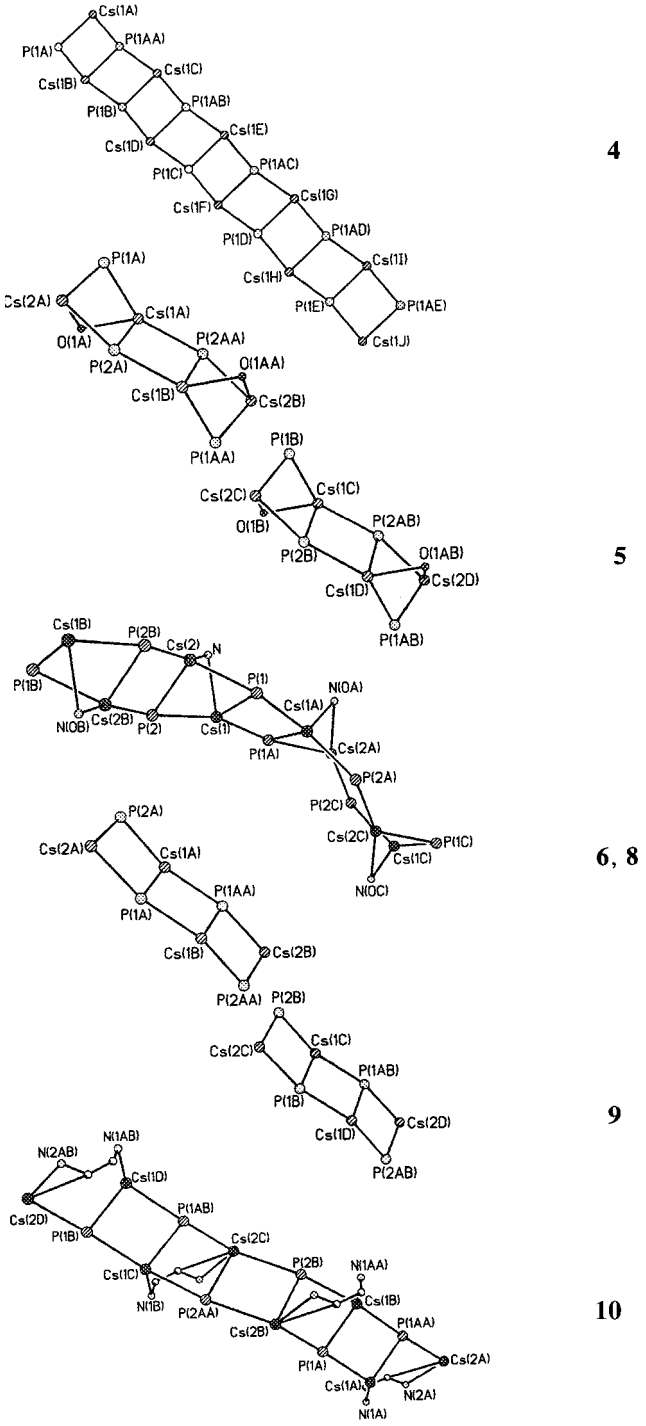

Figure 12. Different kinds of ladders that occur for the structural motifs in the cesium derivatives **4**, **5**, **6**, **8**, **9**, and **10**, in similar orientations.

C(1) and C(21)] above the plane formed by the other five carbon atoms of the phenyl ring. Nonplanarity of the supermesityl aryl ring has been observed as well in other systems, presumably resulting from steric hindrance.[24]

The deviations of the phosphorus atoms in complexes **2**−**10** from the least-squares planes of the phenyl rings are relatively large, namely 0.44 Å (**2**), 0.70 Å (**3**), 0.74 Å (**4**), 0.48 and 0.01 Å (**5**, P(1) and P(2), respectively), 0.58 and 0.38 Å (**6**, P(1) and P(2), respectively), 0.41 and 0.50 Å (**7**, P(1) and P(2), respectively), 0.40 and 0.48 Å (**8**, P(1) and P(2), respectively), 0.52 and 0.05 Å (**9**, P(1) and P(2), respectively), and 0.41 and 0.17 Å (**10**, P(1) and P(2), respectively).

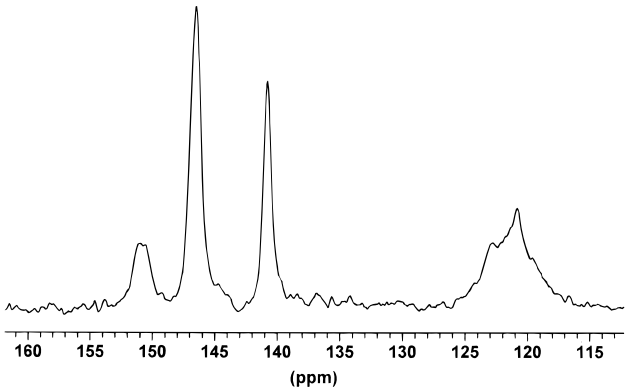

Figure 13. Aromatic region of the ^{13}C CP/MAS NMR spectrum of $[KP(H)^tBu_3Mes]_x$ (**2**).

Solution NMR Spectroscopy. The ^{31}P NMR spectra of complexes **1**−**4** in deuterated tetrahydrofuran at room temperature show a steady and almost linear downfield shift for the P−H doublet ranging from −110.0 ppm (M = Na) to −69.2 ppm (M = Cs). Interestingly, the corresponding lithium derivative is found at a chemical shift of −108.3 ppm, thereby not following the trend of the heavier congeners. The solution structure of the $MP(H)^tBu_3Mes$ species is not clear. However, the observation of a different chemical shift in the case of the lithium derivative indicates that its solution structure and/or solvation mode is supposedly different from those of the heavier alkali metal derivatives of supermesitylphosphane.

Analogously, a downfield shift of the *ipso* carbon atom is observed in the ^{13}C NMR spectrum in tetrahydrofuran solution going from the sodium complex **1** (δ = 155.7 ppm), the potassium derivative **2** (δ = 158.5 ppm), and the rubidium species **3** (δ = 159.4 ppm) to the cesium analogue **4** (δ = 162.5 ppm). The *ipso* carbon atom of the lithium derivative in tetrahydrofuran is observed at 155.0 ppm, thereby matching in general the trend that was observed earlier for the ^{31}P NMR signals. This downfield shift is seen to increase more for the larger atomic radii. Interestingly, all other ^{13}C resonances of the $MP(H)^tBu_3Mes$ derivatives (M = Li−Cs) were found to be basically identical (within the error limits of the determination), which does oppose the idea of increasing effective metal to ring π interaction *in solution.* An obvious trend can be seen from these data, namely that the phosphorus atom and the *ipso* carbon atom become more and more deshielded from the sodium to the cesium derivative.

In light of the fact that the cesium derivative **4** shows a limited solubility in aromatic solvents at room temperature, we decided to use this particular complex for investigating changes in the chemical shift of the phosphorus atom in different solvents. A comparison of the ^{31}P NMR spectra of the cesium derivative **4** reveals a considerable and steady upfield shift going from relatively nonpolar benzene (δ = −65.8 ppm) to more polar and more basic tetrahydrofuran (δ = −69.2 ppm) and to strongly polar and basic pyridine (δ = −73.1 ppm). A comparison of the ^{13}C signals of the *ipso* carbon atom of **4** using tetrahydrofuran (δ = 162.5 ppm) and pyridine (δ = 161.1 ppm) as solvents show a similar trend. Due to the limited solubility of complex **4** in aromatic solvents at room temperature, we failed to detect any signals in the ^{13}C NMR spectrum. It can be concluded from these data that apparently the phosphorus atom is less deshielded in an NMR spectroscopic sense using more polar solvent media.

Solid-State NMR Spectroscopy. We were interested in discovering how solution and solid-state NMR data of complex

2 compare. In particular, we wanted to investigate whether the observation of different K···C and K−P distances found in the molecular structure of complex **2** can further be corroborated using solid-state NMR spectroscopy. Therefore, both a ^{31}P MAS and a ^{13}C CP/MAS study of **2** were undertaken.

Figure 13 shows the aromatic region of the ^{13}C CP/MAS spectrum of the potassium derivative **2** featuring four signals at 151, 146.6, 140.8, and 122 ppm. The broad signal at 122 ppm was definitely identified as corresponding to the *meta* carbon atoms using dipolar dephasing (nonquaternary suppression) techniques. On the basis of integration data combined with a comparison with the solution spectrum, the signal at 151 ppm, exhibiting a poorly resolved doublet structure due to direct coupling to the phosphorus atom, can be assigned to the *ipso* carbon atom. Finally, a comparison with chemical shifts of the signals from the solution spectrum suggests that the two remaining signals correspond to the *ortho* (146.6 ppm) and the *para* (140.8) carbon atoms. This assumption is further corroborated by integration data.

In addition to the four signals in the aromatic region, four more signals are found in the ^{13}C CP/MAS spectrum corresponding to the tertiary carbon atoms (34.8 and 38.7 ppm) and the methyl carbon atoms (31.6 and 32.4 ppm) of the *tert*-butyl groups of the supermesityl ligand. With respect to their chemical shifts, these signals are found at positions similar to those of the corresponding signals from the solution spectrum in deuterated tetrahydrofuran at room temperature.

The ^{31}P MAS NMR spectrum of the potassium salt **2** exhibits a signal at −104 ppm. A comparison of this signal with the corresponding solution NMR spectrum recorded in deuterated tetrahydrofuran at room temperature reveals a low-frequency shift (approximately 15 ppm) for the solid-state NMR spectrum.

Conclusion

Our study provides detailed insight into structural aspects of a number of systems of heavier alkali metal congeners of supermesitylphosphane with respect to structural changes that result from different alkali metal cation/solvent combinations employed in the crystallization process. This work demonstrates that the structural motif found in molecular species of heavier congeners of alkali metal phosphides depends on the size of the alkali metal cation, as well as on the donor solvents employed for crystallization. Ladder-type structures are found to be typical for this class of compounds.

Use of the sterically demanding supermesityl ligand permits the syntheses and structural characterizations of several alkali metal phosphides which exhibit novel structural motifs in the solid state. Also, it is demonstrated that these species can be easily prepared in good yields thereby representing potential transfer agents for the −P(H)^{t}Bu$_3$Mes ligand. Further investigations in this area of chemistry are clearly warranted.

Acknowledgment. This work was supported by the Fonds der Chemischen Industrie and the Leonhard-Lorenz foundation. Generous support from Professor H. Schmidbaur is gratefully acknowledged. The University of Delaware acknowledges the National Science Foundation for support of the purchase of the CCD-based diffractometer (Grant CHE-9628768).

Supporting Information Available: X-ray crystallographic files, in CIF format, for the structure determinations of complexes **3**−**10** are available on the Internet only. Access information is given on any current masthead page.

Note Added in Proof

While our manuscript was in the review process, a sterically congested cesium phosphide derivative was reported: Driess, M.; Pritskow, H.; Skipinski, M.; Winkler, U. *Organometallics* **1997**, *16*, 5108.

IC971178Y